Biogeochemical behaviour of geogenic As in a confined aquifer of the Sologne region, France

Fabienne Battaglia-Brunet, Aude Naveau, Lise Cary, Maïté Bueno, Justine Briais, Mickael Charron, Catherine Joulian, Hugues Thouin

Biogeochemical behaviour of geogenic As in a confined aquifer of the Sologne region, France

Battaglia-Brunet Fabienne, Naveau Aude, Cary Lise, Bueno Maïté, Briais Justine, Charron Mickael, Joulian Catherine, Thouin Hugues

PII: S0045-6535(22)01745-3

DOI: https://doi.org/10.1016/j.chemosphere.2022.135252

Reference: CHEM 135252

To appear in: *ECSN*

Received Date: 9 February 2022

Revised Date: 28 May 2022

Accepted Date: 3 June 2022

Please cite this article as: Fabienne, B.-B., Aude, N., Lise, C., Maïté, B., Justine, B., Mickael, C., Catherine, J., Hugues, T., Biogeochemical behaviour of geogenic As in a confined aquifer of the Sologne region, France, *Chemosphere* (2022), doi: https://doi.org/10.1016/j.chemosphere.2022.135252.

Credit author statement

Battaglia-Brunet Fabienne, Conceptualisation, Methodology, Writing – original draft, Funding acquisition, Naveau Aude, Conceptualisation, Investigation, Writing – review and Editing, Cary Lise, Conceptualisation, Data processing, Writing – review and Editing, Funding acquisition, Bueno Maïté, Investigation, Writing – review and Editing, Briais Justine, Investigation, Writing – review and Editing, Charron Mickael, Investigation, Joulian Catherine, Investigation, Writing – review and Editing, Thouin Hugues, Conceptualisation, Methodology, Investigation, Data processing, Writing – review and Editing.

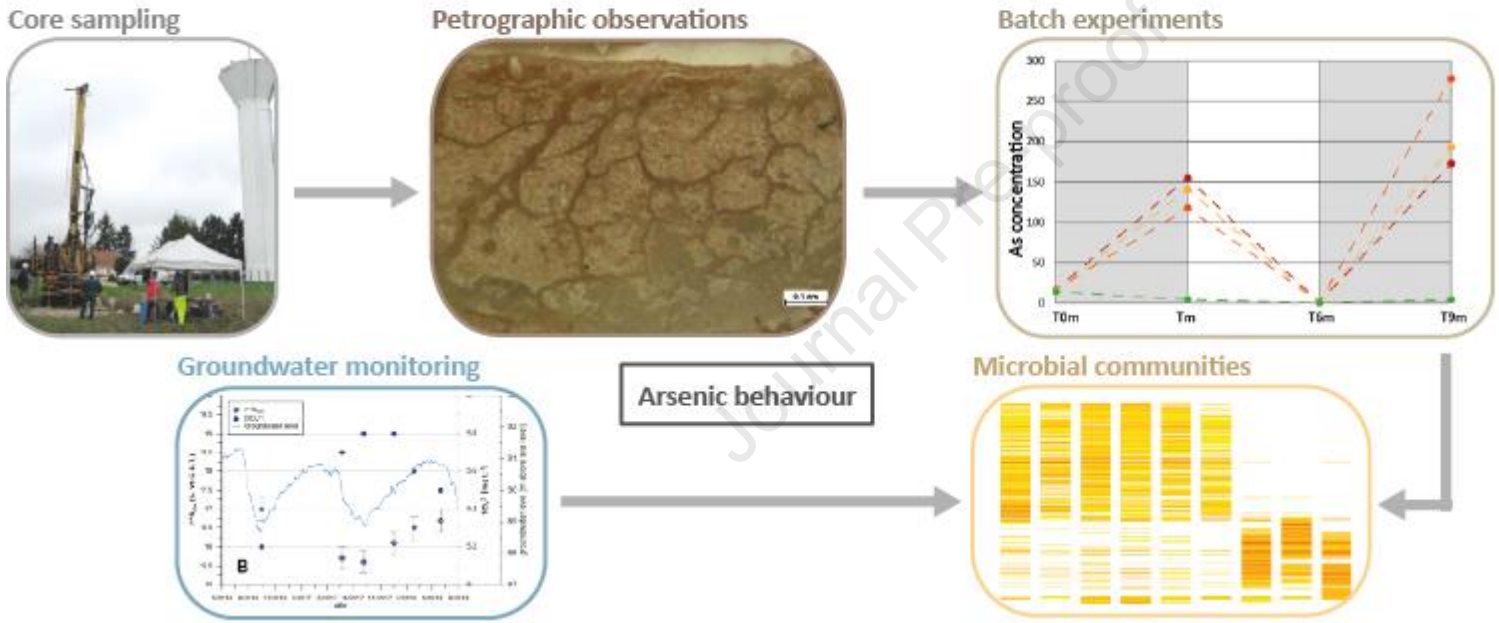

Biogeochemical behaviour of geogenic As in a confined aquifer of the Sologne region, France

Battaglia-Brunet Fabienne[1, 2], Naveau Aude[3], Cary Lise[4], Bueno Maïté[5], Briais Justine[1], Charron Mickael[1], Joulian Catherine[1], Thouin Hugues[1]

[1] BRGM, F-45060 Orléans, France

[2] ISTO, UMR7327, Université d'Orléans, CNRS, BRGM, F-45071 Orléans, France

[3] Institut de Chimie des Milieux et Matériaux de Poitiers (IC2MP), Université de Poitiers/CNRS, UMR 7285, Bâtiment B8, rue Michel Brunet, F-86022 Poitiers Cedex, France

[4]BRGM, F-59810 Lesquin, France

[5] Universite de Pau et des Pays de l'Adour, E2S UPPA, CNRS, Institut des Sciences Analytiques et de Physicochimie pour l'Environnement et les Matériaux-IPREM, UMR5254, 64000 Pau, France

ABSTRACT

Arsenic (As) is one of the main toxic elements of geogenic origin that impact groundwater quality and human health worldwide. In some groundwater wells of the Sologne region (Val de Loire, France), drilled in a confined aquifer, As concentrations exceed the European drinking water standard (10 µg L^{-1}). The monitoring of one of these drinking water wells showed As concentrations in the range 20 to 25 µg L^{-1}. The presence of dissolved iron (Fe), low oxygen concentration and traces of ammonium indicated reducing conditions. The $\delta^{34}S_{SO4}$ was anticorrelated with sulphate concentration. Drilling allowed to collect detrital material corresponding to a Miocene floodplain and crevasse splay with preserved plant debris. The level that contained the highest total As concentration was a silty-sandy clay containing 26.9 mg kg^{-1} As. The influence of alternating redox conditions on the behaviour of As was studied by incubating this material with site groundwater, in biotic or inhibited bacterial activities

conditions, without synthetic organic nutrient supply, in presence of H_2 during the reducing periods. The development of both AsV-reducing and AsIII-oxidising microorganisms in biotic conditions was evidenced. At the end of the reducing periods, total As concentration strongly increased in biotic conditions. The microflora influenced As speciation, released Fe and consumed nitrate and sulphate in the water phase. Microbial communities observed in groundwater samples strongly differed from those obtained at the end of the incubation experiment, this result being potentially related to influence of the sediment compartment and to different physico-chemical conditions. However, both included major Operating Taxonomic Units (OTU) potentially involved in Fe and S biogeocycles. Methanogens emerged in the incubated sediment presenting the highest solubilised As and Fe. Results support the hypothesis of in-situ As mobilisation and speciation mediated by active biogeochemical processes.

Key words: groundwater, arsenic, speciation, microbial communities, sediment incubation, changing redox

1. Introduction

The presence of arsenic (As) in groundwater is a widespread environmental issue which consequences affect millions of people's health (Ravenscroft et al., 2009; Chakraborti et al., 2016). Chronic exposure to As was reported to increase the risk of a range of illnesses including cancer (Schmidt, 2014; Tsuji et al., 2019). High As concentrations exceeding the European drinking water standards (10 µg L^{-1}, EU Council Directive 98/83/EC) are generally linked to geological context in many regions of the world (Podgorski and Berg, 2020). This toxic element presents several oxidation states and compounds potentially changed by microbial activities according to redox conditions. Arsenic release in several sedimentary and alluvial aquifers is

linked with low redox conditions (Ravencroft et al. 2009; Erickson et al., 2019) and reductive reactions catalysed by microbial processes (Deng et al., 2018). These bio-reactions are linked to the availability of electron donors, generally organic matter. Several studies reported the mobilisation of As from underground sediments fuelled by organic pollutants plumes (Erickson et al., 2016; Ziegler et al., 2017). However, the natural organic matter present in sediments, found both in active and ancient floodplains, also plays the role of electron donor in reactions that solubilise As (Sahu and Saha, 2015; Johannesson et al., 2019). The reductive dissolution of As-bearing FeIII oxides minerals was evidenced as one of the main bio-processes able to release As from sediments to groundwater (Welch et al., 2000; Nath et al., 2009; Duan et al., 2019). However, sulphur biogeocycle may also influence As behavior: dissolved sulphide can contribute to FeIII reduction (Wang et al., 2014) and As may be adsorbed on FeS precipitates. Moreover, the formation of soluble thio-As complexes may increase As mobility through decreasing the adsorption of As on solid oxides (Pi et al., 2018). Several studies described the strong link between As, Fe and S biogeochemical cycles and As mobility and proposed geochemical models (Wang et al., 2014; Pi et al., 2018). Influence of the bio-reduction of iron oxides and sulphate on As concentrations, related with fluctuations of groundwater level and redox conditions, was observed (Schaefer et al., 2016; Zheng et al., 2020). Functional diversity of As-rich groundwater supported these hypotheses by the presence of microorganisms able to reduce AsV, either through AsV respiration or resistance mechanisms, AsIII-oxidising bacteria, FeIII-reducing and SO_4-reducing bacteria (Paul et al., 2015; Cavalca et al., 2019; Zheng et al., 2019; Wang et al., 2021). In addition to field studies, a range of laboratory experiments were focused on the elucidation of biogeochemical processes in sediments from floodplains and deltas. Mechanisms of As release were studied through long-term (Radloff et al., 2007; Gillipsie et al., 2016; Duan et al., 2019; Gao et al., 2021) or short-term (Schaefer et al., 2016) incubations of underground sediments. Electron donors supply generally enhanced As release in biotic and

anoxic conditions (Gillipsie et al., 2016; Wang et al., 2017; Deng et al., 2018), however results strongly depended on the sediment geochemistry (Deng et al., 2018). Arsenic mobility was hampered in presence of oxygen (Radloff et al., 2007) and mobilised during anoxic periods when redox conditions were alternated (Duan et al., 2019). Microbial communities of incubated sediments were rarely described, although studies performed with core materials from the alluvial Jianghan plain in the middle reaches of the Yangtze River (China) indicated the presence of both FeIII- and SO_4-reducing bacteria in anaerobic microcosms showing As release (Duan et al., 2019; Gao et al., 2021). However, complementary information on the influence of microbial community structure and activity on the amplitude of the bio-reactions mobilising As would help to improve models that predict changes in groundwater quality. In this context, the present research aimed to clarify the links between microbial processes and As release in groundwater, through the example of the Sologne region (Val de Loire, France), where As concentrations exceeding 10 µg L^{-1} were detected in 43 wells out of 135 that have been monitored (Supplementary Figure 1, https://ades.eaufrance.fr/), distributed in an area of approximately 5 000 km^2, in a geological context of Miocene sedimentary formation (Cary et al., 2018). A drinking water well was monitored for two years, in order to study the evolution of water parameters. In parallel, core sediment material was characterised for mineralogy and geochemistry, then incubated in alternating redox conditions. Determination of microbial indicators and comparison of the evolution of physico-chemical parameters in biotic and abiotic conditions were performed to enlighten the biogeochemical processes influencing the mobility and speciation of arsenic.

2. Materials and Methods

2.1. Study site and sampling

The sampling site is located on the territory of Marcilly-en-Gault village, in Sologne (Supplementary Figure 1), a wetland-rich region in the center of France, South of Orleans city,

where sands and clays of continental detrital origin (Burdigalian, Miocene) cover the calcareous aquifer of the Orléanais (Aquitanian, Miocene, Deprez and Martin, 1970). Water samplings were performed in the drinking water well (reference BSS 04611X0001/FAEP, BSS001FRCU, http://ficheinfoterre.brgm.fr/InfoterreFiche/ficheBss.action?id=04611X0001/FAEP), drilled in 1965, at 90.2 m total depth, the water level being at 21 m depth (without pumping) and the pumping performed at 70 m depth (from the ground surface). Total historical regulatory monitoring since 1986 indicates median As concentration of 23.0 µg L^{-1} with a standard deviation of 4.7 µg L^{-1}. Well water was sampled after pumping sufficiently to reach stable values of pH, redox potential, dissolved oxygen concentration and conductivity. Five sampling campaigns were performed at the following dates: June 2017 23th; September 2017 4th; December 2017 18th; February 2018 27th, May 2018 29th. Water samples were filtrated at 0.45 µm (except for total organic carbon) and conditioned for further chemical analyses (Supplementary table 1).

For molecular microbiological analyses, 10 L of groundwater were sampled at each sampling date in 2 L sterile polyethylene bottles, kept on ice until filtration at the laboratory within 12 hours after sampling. Water samples were filtrated on sterile 0.22 µm nitrocellulose filters, that were immediately stored at -20°C until microbial DNA extraction.

Core sampling was performed about 100 m North from the location of the well, with an auger drilling machine (diameter 152 mm) (Supplementary Figure 1B). Core was performed down to 48.5 m depth, in March 2017 (23-24th) without adding drilling fluid. Samples of each different geological facies were subsampled on-site with an alcohol-washed spatula, and immediately stored in sterile glass jars, flushed with N_2, and kept on ice until storage at 4°C in the laboratory. Jars for microbial analysis and experiments were always opened in sterile conditions. Samples for chemical and mineralogical analyses were kept frozen (-20°C) until analyses.

2.2. Mineralogical and petrographic analysis

Core samples were lyophilised and milled below 200 µm. Powder samples (infra 50 µm fraction) were analysed by X-ray diffraction (XRD) using a Phillips Panalytical X'Pert Pro apparatus in the same experimental conditions as described by Bassil et al. (2016). Phase identification was made with the X'pert HighScore software using JCPDS Pdf2 mineralogical database (Supplementary Figure 5). After deconvolution and integration of the main peak area of each phase using Fytyk software, the semi-quantifications (Supplementary Table 5) were realised by applying modified RIR method (Chung, 1975).Thin sections (26 mm × 46 mm) were consolidated after impregnation at room temperature and under atmospheric pressure with a two-component epoxy resin (Araldite 2020) and 20% acetone. The thin sections were observed using an optical polarised light microscope (Nikon Eclipse E600 POL).

2.3. Batch experiments

Incubations of core solids sampled at 31.5 m depth, named M8, were prepared in 1 L-Shott bottles equipped with rubber stoppers and sterilised by autoclaving. Each batch was composed of 60 g solids and 600 mL of groundwater from the drinking water well (sampled on May 2018 29th). One batch was prepared with M8 core material submitted to γ-irradiation (Dagneux, France) in order to observe the evolution of the system when biological activities are inhibited (IN condition). The water was used as it was pumped for biotic experiments (BIO condition), and filtrated at 0.22 µm to remove bacteria for the IN condition. Three BIO flasks were prepared by distributing a single slurry of core sediment mixed with site water (magnetic stirring) in 3 bottles with a 25 mL sterile pipette. Alternate redox conditions were applied as follows: 3 months in anaerobic conditions (T0m to T3m), followed by 3 months in aerobic conditions (T3m to T6m) then again 3 months in anaerobic conditions (T6m to T9m). At the beginning of each anaerobic periods, the gas phase composition was imposed at 75% N_2, 25% H_2, and 1.25% CO_2, at a total pressure of 1 bar over the atmospheric pressure. For establishing the intermediary aerobic conditions, the flasks were opened in order to replace the $N_2/H_2/CO_2$ mixture by sterile

air. Flasks were incubated at 20°C under reciprocal agitation. Sampling at the end of each anaerobic period was performed in a glovebox (N_2 atmosphere) under agitation, in order to avoid change of the solids/water ratio. Just after sampling, pH, redox potential and conductivity were immediately measured. Samples (10 mL) were filtrated at 0.22 µm in a sterile Hungate tube filled with N_2 and kept at 4°C until As speciation. Samples (15 mL) filtrated at 0.45 µm were acidified with HNO_3 for analyses of total As and major cations. Samples (15 mL) filtrated at 0.45 µm but not acidified were kept for quantification of major anions (nitrate, sulphate). Slurry samples (1 mL) were stored in sterile tubes for Most Probable Number (MPN) of As-transforming microbes analyses. At the end of experiment, slurries were centrifuged in sterile falcon tubes, and the pellets containing both bacteria attached on sediments and suspended in water were stored at -20°C until microbial DNA extraction.

2.4. Chemical analyses

Methods for analysing major chemical species and trace elements in water from the site and incubations are detailed in Supplementary Table 1. Separation of As species in groundwater samples was performed on site (Kim et al., 2001). This method gives precise AsIII and AsV concentrations when only these two species are present, thus results are given as AsIII-like and AsV-like species, because other As forms might be present in groundwater. Isotopy of sulphur ($\delta^{34}S$) was measured by continuous flow isotope ratio mass spectrometry (CF-IRMS) after precipitation as $BaSO_4$ and reduction/pyrolysis (Kloppmann et al., 2018). The total elemental composition of the core samples (Table 2) was determined, after digestion (HNO_3/HF), by ICP-OES and ICP-MS in an accredited laboratory (CRPG-CNRS, Nancy). Organic carbon concentrations were determined by CHNS analysis (Flash 2000 Thermo, IC2MP, France). Total As and Se were determined by ICP-MS equipped with an octopole collision/reaction cell (C/RC) (Agilent 7500ce) after HNO_3/HCl digestion. The C/RC was pressurised with helium and hydrogen delivered at 1 and 4 mL min^{-1}. Analyses of major cations and anions in water

samples from incubation experiments were performed by ion chromatography equipped with conductivity detectors (Professional IC Vario, Metrohm). Anions were separated with a Metrosep A Supp 16 ionic resin column (150 mm × 4 mm) and cations with a Metrosep C6 (150 mm × 4 mm). Speciation of As in these samples was performed by HPLC (Agilent 1100 series HPLC pump) coupled to ICP-MS (Agilent 7500ce) with the same C/RC operating conditions as described for total analysis. Chromatographic separation was carried on using an anion exchange stationary phase (Agilent G3154-65001 column and G3154-65002 guard column) with an ammonium nitrate mobile phase (20 mmol L^{-1}, 2.5% (v/v) methanol and pH 8.5 adjusted with ammonia), delivered at 1 mL min^{-1} flow rate. The sample injection volume was 100 µL. These analytical conditions allow the separation of AsIII, AsV and mono- and di-methylated AsV species (MMA^V and DMA^V) (see example chromatogram in Supplementary Figure 2).

2.5. Microbiological analyses

2.5.1. MPN of AsIII-oxidising and AsV-reducing bacteria

Most Probable Numbers (MPN) of active AsIII-oxidising and AsV-reducing microbes were determined in slurries by the methods described in Thouin et al. (2016) and Thouin et al. (2018), with the following modification: the pH of the culture media was adjusted to 7 in order to fit with the groundwater pH.

2.5.2. Microbial DNA extraction

Microbial DNA was extracted from (i) the filters obtained from groundwater filtration and stored at -20°C, cut into strips with a sterile scalpel just prior extraction, and (ii) the slurries pellets from end of batch experiments. The FastDNA™ Spin Kit for Soil procedure (MP Biomedicals) was followed, using a FastPrep-24™ instrument at a speed of 5 m s^{-1} for 30 s.

198 DNA extract concentration was measured using the Quantifluor dsDNA sample kit and the
199 Quantus fluorimeter, according to the manufacturer's recommendations (Promega).

200 *2.5.3. 16S rRNA, aioA and arsB genes copy number monitoring*

201 Abundance of bacterial 16S rRNA genes and of *aio*A and *ars*B functional genes, encoding
202 respectively for the catalytic subunit of arsenite oxidase and the AsIII-efflux pump of Ars
203 resistance system, were performed by quantitative PCR (qPCR). The main characteristics of
204 qPCR reactive mixtures and programs are described in Supplementary Information 1,
205 Supplementary Table 2, and in Michel et al. (2021), Fernandez-Rojo et al. (2017) and Poirel et
206 al. (2013).

207 *2.5.4. 16S rRNA gene metabarcoding*

208 For next generation sequencing, amplicon libraries and sequences were generated by INRAE
209 Transfert (Narbonne, France). Briefly, the V4-V5 region of the gene coding 16S rRNA (bacteria
210 and archaea) was amplified using the barcoded, universal primer set 515WF/918WR (Wang et
211 al., 2009). PCR reactions were performed using AccuStart II PCR ToughMix kit and cleaned
212 (HighPrep PCR beads, Mokascience). Pools were submitted for sequencing on Illumina MiSeq
213 instrument at GeT-PlaGe (Auzeville, France). Sequences were processed using the FROGS
214 (v.3.2) bioinformatics pipeline (Escudié et al., 2018), implemented into the Genotoul plateform
215 of the Galaxy server of Toulouse (details in Supplementary information 1). The raw datasets
216 are available on the European Nucleotide Archive system under project accession number
217 PRJEB53046.

218

219 *2.5.5. Statistical analyses*

220 Statistical tests were carried out using R 4.0.3 (www.r-project.org). Redundance analysis
221 (RDA) with the vegan R package, was performed to identify the effects of environmental
222 variables on bacterial composition structure, based on the relative abundance of the detected

OTUs in water sample from the temporal evolution. This analysis was calculated based on Hellinger - transformed phylum abundance basis of 16S rRNA gene data (Borcard et al., 2011). Environmental explanatory tested variables were standardised and the function ordistep in vegan package was used to identify the significant explanatory forward environmental variable. The significance of the RDA model was tested by ANOVA based on Monte Carlo test with 999 permutations. This analysis helps to determine the most influential factors and the extent that various environmental parameters affected bacterial phylum, most abundant OTU composition. Principal component analysis (PCA) was performed on biogeochemical parameters from the batch experiment.

3. Results

3.1. Temporal monitoring of groundwater

3.1.1. Groundwater level and geochemistry

The groundwater level variations (Fig. 1A and B) present well-marked annual cycles with high level observed in late spring and the lowest level in late summer. The total amplitude of these

variations is in the range of 2 to 3 m.

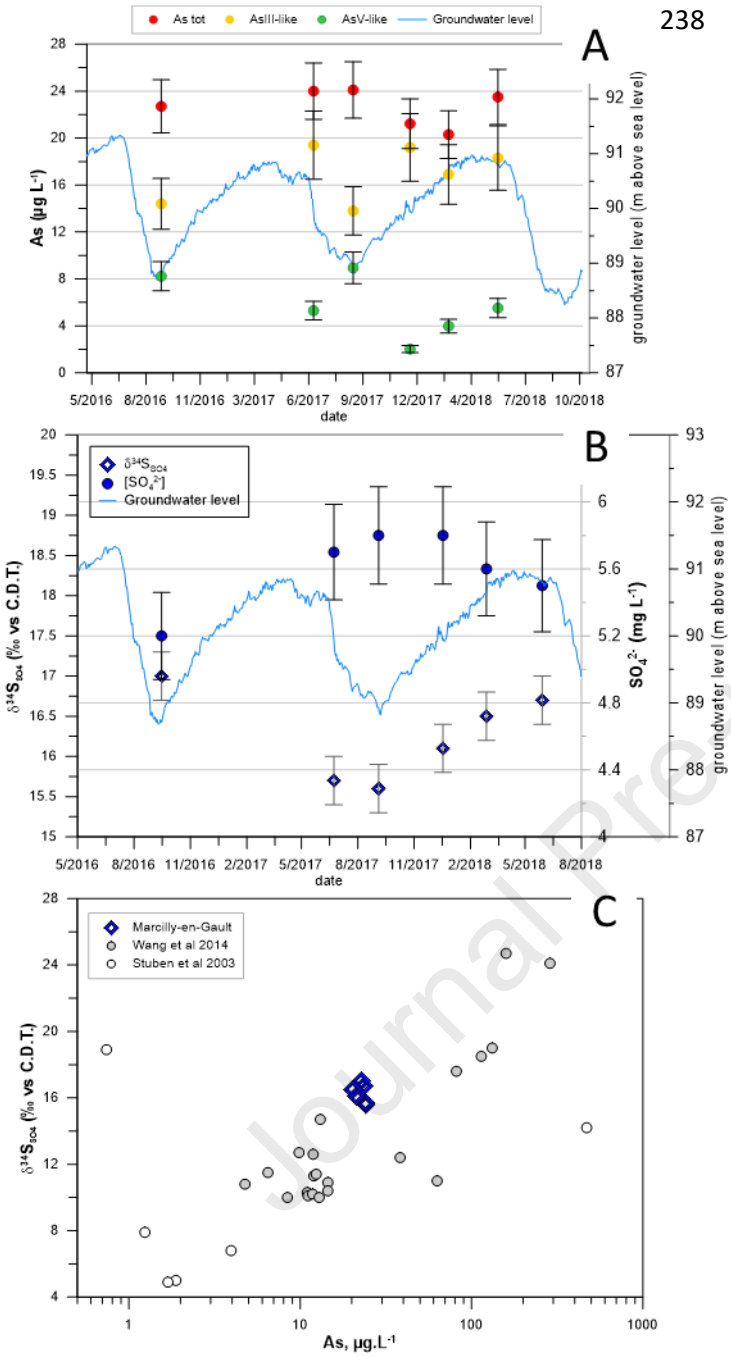

Fig. 1. Evolution of groundwater geochemical parameters: (A) Total As (red) and As speciation i.e. on site separation of AsIII- (yellow) and AsV- (green) like species (error bars indicate the measurement uncertainty, and groundwater level (IGN French national altitude reference, https://ades.eaufrance.fr/) corresponding to the control well referenced 04612X0024/F (BSS001FRES) located 1.4 km from the drinking well; (B) $\delta^{34}S$ (open symbol) in SO_4 and SO_4 concentration (closed circles), error bars indicate the analytical standard deviation; and

246 groundwater leveland (C) evolution of $\delta^{34}S$ with total As concentration including data from
247 previous studies.

248

249 The total As concentration (Fig. 1A) remained between 20 and 25 µg L^{-1} along the monitoring
250 period, with a mean of 23.6 µg L^{-1} and a standard deviation of 1.6 µg L^{-1}, lower than the
251 measurement uncertainty (2.0-2.5 µg L^{-1}). The speciation of As seemed to be more variable
252 than total As concentration. Dissolved Fe concentration varied between 0.15 and 0.3 mg L^{-1} (±
253 35%), and SO_4 concentration between 5.2 and 5.8 mg L^{-1} (± 5%). Ammonium was always
254 detected, with concentrations generally in the range 0.07-0.1 mg L^{-1} (± 40%, Supplementary
255 Tables 1 and 3). For these three parameters, the temporal variations remained in the range of
256 the analytical measurement uncertainty. Results of isotopic analyses of SO_4-S showed
257 variations of $\delta^{34}S$ higher than the range of analytical standard deviation (Fig. 1B).

258

259 *3.1.2. Microbial parameters*

260 Rarefaction curves (Supplementary Figure 3) together with richness and diversity indexes
261 (Supplementary Table 4) indicated a relatively low bacterial diversity. Bacterial communities
262 of the groundwater were composed of a majority of Proteobacteria (Fig. 2A). The most
263 abundant OTU found in groundwater was affiliated to Hydrogenophilaceae family, with an
264 unknown genus representing 69 to 86% of the total sequences (Fig. 2B). The second main OTU
265 belonged to the Gallionellaceae family, gathering autotrophic FeII-oxidisers (Hallbeck and
266 Pedersen, 2014). Autotrophic bacteria using FeII as energy source, identified at the genus level,
267 (*Gallionella*, *Ferriphaselus* and *Sideroxydans* genera), were always present in groundwater
268 samples (from 0.5 to 2.2 % of the sequences). Sulphate-reducing bacteria (SRB), including
269 *Desulfovibrio* and *Desulfatirhabdium* genera were always present but in small abundance (total
270 from 0.1 to 0.5 % of the sequences), and this abundance did not vary with seasons. Bacteria

involved in denitrification and able to use sulphur compounds as energy source, identified at the genus level (*Sulfuritalea*, *Denitratisoma*, *Sulfuricella*) were always present as minor OTUs (total from 0.01 to 0.1% of the sequences) in groundwater. The global abundance of the universal bacterial 16S rRNA gene did not follow a clear seasonal tendency (Fig. 2C). The two functional genes, i.e. *aio*A and *asr*B genes, involved in As biotransformations were always present, and their abundance ranged between 1.6×10^6 and 2.6×10^8 gene copies L^{-1} for *aio*A, and between 5.8×10^3 and 2.2×10^5 gene copies L^{-1} for *ars*B. .

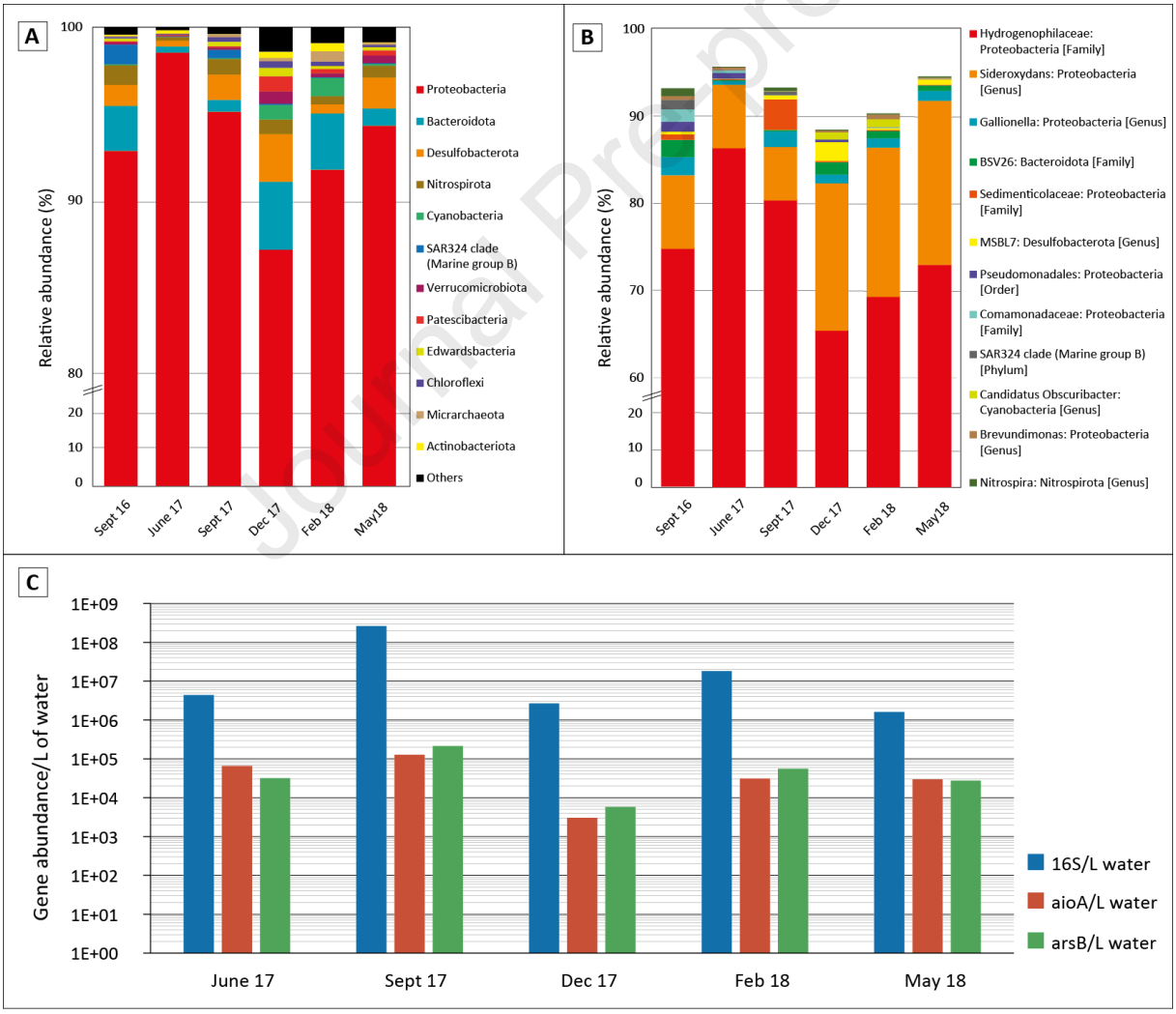

Fig. 2. Drinking water well of Marcilly-en-Gault, evolution of (A) main bacterial phyla; (B) most abundant OTUs; (C) total biomass (16S rRNA gene copies) and functional genes *aio*A and *ars*B copies respectively involved in the biological oxidation and reduction of arsenic.

A RDA was performed to identify the influence on microbial community structure of physico-chemical characteristics of groundwater (Fig. 3). The results indicated that total As, total Fe and dissolved oxygen concentration were explanatory variables that significantly influenced the community structure at the phylum level (Fig. 3A), whereas only Mn concentration significantly influenced the community structure at the genus level (Fig. 3B).

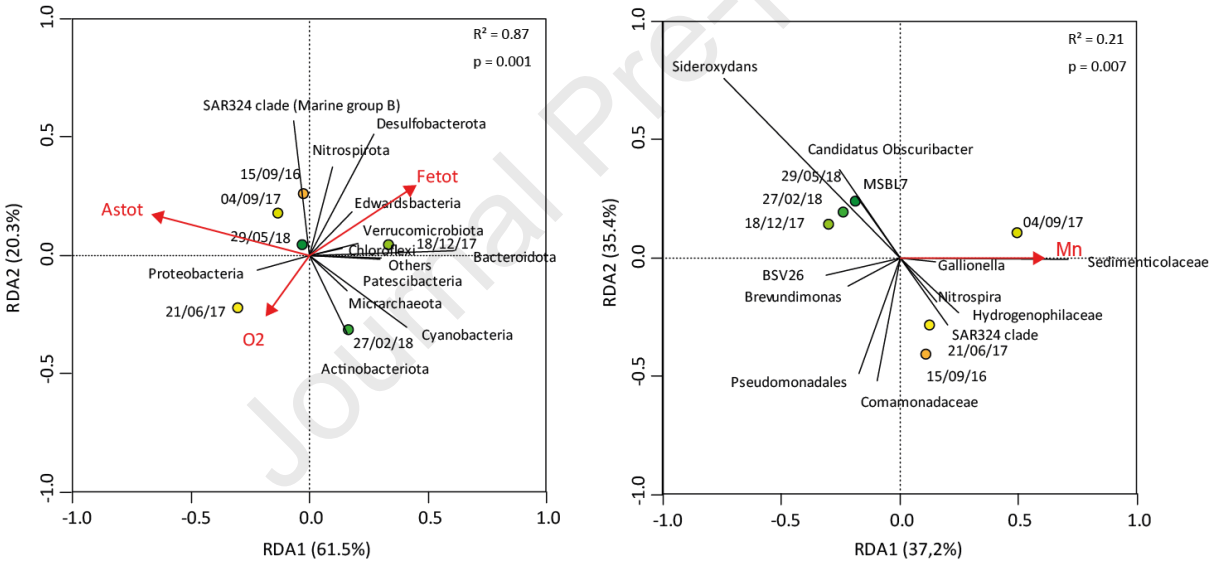

Fig. 3. RDA of sequence abundance assigned at phylum level (A) and genus level (B) of microbial communities in groundwater samples in relation to environmental variables. Red lines represent the significant environmental variables, black lines represent the phylum or genus and circles represent the samples, from orange to dark green following the chronology.

3.2. Solids description

3.2.1. Sedimentological description

296 The sedimentological description (Supplementary Figure 4) begins at 13.5 m depth; this section
297 shows at the base the dominant clays with roots traces and plant debris (48.0 m to 35.5 m).
298 These clays are followed by poorly sorted medium and coarse sands (35.5 m to 31.5 m). Finally,
299 the youngest levels (31.5 m to 13.6 m) correspond to an alternation of well-sorted medium
300 sands and clays with plant debris. The profile represents a part of "Sables et Argiles de
301 Sologne" formation (Desprez and Martin, 1970) that covers the aquifer limestone formations
302 "Marne de l'Orléanais" and "Calcaire de Pithiviers ». The sedimentary filling is characterised
303 by clays and heterogeneous sands (well to poorly sorted fine to coarse sands). These clays with
304 root traces, organic matter and plant debris correspond to floodplain deposits. The thick sandy
305 part (poorly-sorted) probably corresponds to meandering channel (river) and the isolated sandy
306 levels (well-sorted) in the floodplain clays corresponds to crevasse splay deposits.

307 *3.2.2. Mineralogy*

308 The mineralogy of the sediments was determined by XRD on 13 different samples
309 corresponding to 13 visually different geological layers, with one of the layer (M9, 37.5 m deep)
310 divided in two sub-samples (XRD spectra given in supplementary Figure 5). Total As
311 concentration was also determined on these samples (Supplementary Table 5). The upper 8
312 layers (M1 – M8) represent a floodplain clays with crevasse splay sands. Two samples, M7 and
313 M8 (floodplain and crevasse splay facies), present the two highest As concentrations of the
314 profile, (> 20 ppm), and relatively high clay content. These two layers are visually characterised
315 by different colours; blue for M7, and red-brown for M8. The M9 layer presents heterogeneous
316 facies, marly in the upper part (M9a). This level is close to the interface between two different
317 geological formations, the sands and clays of Sologne above, and the underlying calcareous
318 formation. The deeper samples (M10-M13) are mostly calcareous facies (M11 and M13) or
319 marl-calcareous (M10 and M12).

320 *3.2.3. Chemical composition*

Three samples, corresponding to the 2 clayey levels with high As concentrations (M7 and M8), and one of the underlying calcareous levels (M12) were characterised in terms of major and trace elements contents (Supplementary Table 6 and Fig. 4 for M8). These analysis confirmed the siliceous feature of M7 and M8 compared with the characteristics of M12 that defined this level as calcareous. Iron, sulphur and organic carbon contents were similar in the 3 samples, with significant Fe contents but very low S and C concentrations. Arsenic and metals (Pb and U) were enriched in M7 and M8 compared with M12.

2.3.4. Petrographic description

Petrographic observations of resin-impregnated M8 sample (Fig. 4) showed that the material was mainly composed of beige siliceous clay showing numerous desiccation traces (arrow D in Fig. 4A), and a laminar structure (arrow L in Fig. 4A). Desiccation cracks form sub-polygonal structures where the siliceous matrix can be partially or entirely transformed into clay (Fig. 4B, arrows MA), as indicated by the presence of remaining white matrix in clayey phases (Fig. 4C, D, E). The laminations are composed of successive layers of clear siliceous material and clayey beige material. Small black, dark brown and red pellets are observed inserted into the layers (Fig. 4D).

337

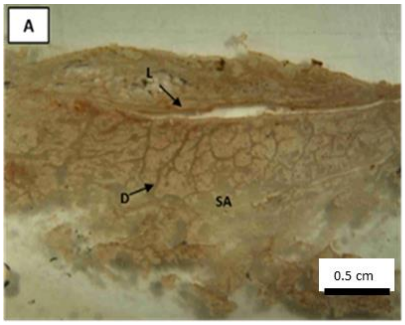

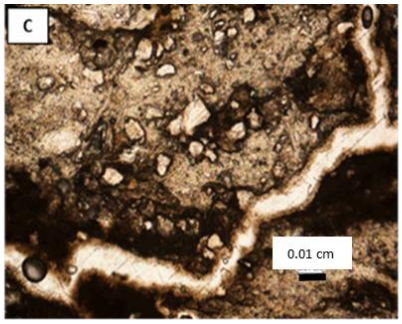

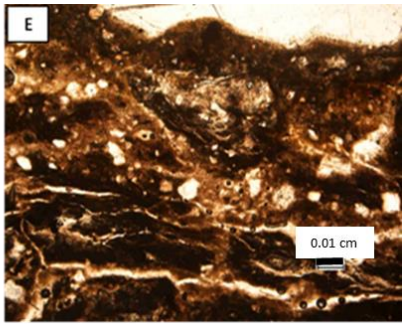

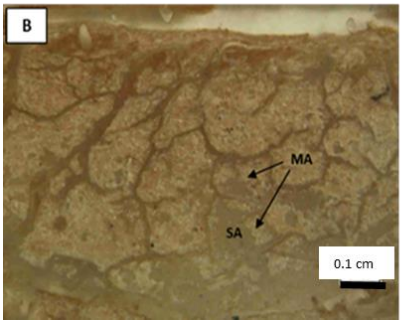

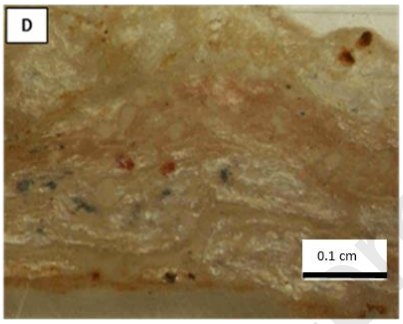

F

SiO_2 (%)	60.3	Na_2O (%)	0.1
Al_2O_3 (%)	17.3	K_2O (%)	1.64
Fe_2O_3 (%)	**5.7**	TiO_2 (%)	1.01
FeO (%)	0.18	**As ppm**	**26.9**
Total S (%)	0.01	Se ppm	1.11
MnO (%)	0.03	Sr ppm	87.1
MgO (%)	1.17	Pb ppm	44
CaO (%)	0.8	U ppm	4.5

338

339 **Fig. 4.** Microscopic petrographic observations of thin sections (A to D) and chemical
340 composition (F) of M8 sample. Letters inside the pictures correspond to: SA:
341 Siliceous/Argillaceous mud; L: Laminar structures; MA: Sub-polygonal structures (partly
342 argillaceous siliceous matrix); D: Desiccation traces.

343 *3.3. Batch experiments with M8*

344 *3.3.1. Water geochemistry*

345 Total As concentrations increased during the anaerobic periods and decreased during the
346 aerobic step in the BIO slurries (Fig. 5). These variations in As concentrations were not
347 observed in the IN condition. At the end of the first anaerobic period (T3m), total As
348 concentrations were in the range 100-150 µg L^{-1} in BIO slurries, and the three parallel
349 microcosms behaved in the same way. Conversely, at the end of the second anaerobic period
350 (T9m), the BIO B slurry presented higher As concentration (275 µg L^{-1}) than A and C (between
351 150 and 200 µg L^{-1}). Total dissolved Fe followed the same evolution as total As, with
352 concentrations close to 900 µg L^{-1} at the end of the first anaerobic period, and up to 7000 µg L^{-}

353 [1] in B slurry at the end of the second anaerobic period. The redox potential was lower at the end
354 of the second anaerobic period in all flasks, independently from the presence of active bacteria,
355 and pH was higher in BIO than in IN conditions all along the experiment. During the anaerobic
356 periods, pH tended to decrease, probably because of CO_2 present in the gas phase. Acidification
357 was less important in B slurry than in A and C, at the end of experiment.

358

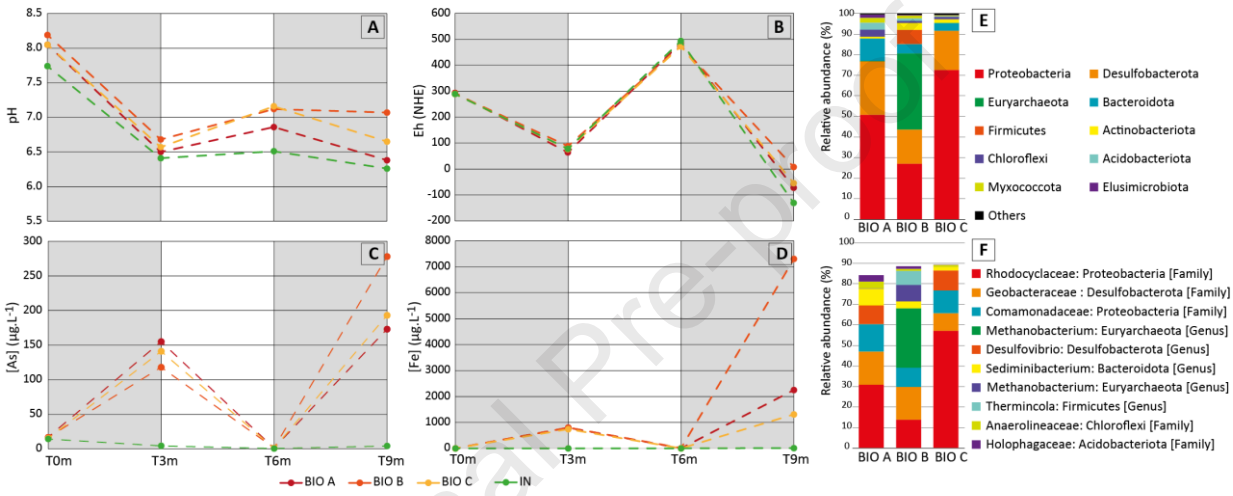

359

360 **Fig. 5.** Evolution of pH (A), redox potential (Eh, B), total As (C) and Fe (D) concentrations in
361 the incubated slurries; anaerobic periods are presented in grey background. IN: inhibited
362 biological activities; BIO: microcosms with active biological activities. T0m: starting up; T3m:
363 3 months; T6m: 6 months; T9m: 9 months. Major phyla (E) and 10 major OTUs (F) found in
364 the BIO slurries at the end of the second anaerobic period (T9m).

365

366 The incubation conditions influenced the speciation of As in the water phase (Table 1). In the
367 IN condition, AsIII was the major initial species, then AsV became the main form of As until
368 the end of experiment. In the BIO condition, at the end of the anaerobic periods, As-containing
369 species were detected, with retention times that did not match any available standard. They
370 could not be precisely quantified because of the lack of standards, however as estimated based

371 on AsV standard additions slope, they represented more than 50% of total As in A, B and C at
372 the end of the first anaerobic period and in A and C at the end of the second anaerobic period.
373 The unidentified As species were not detected at the end of the aerobic incubation period,
374 however at the end of this experimental step, dimethyl-arsenate (DMA^V) was present in BIO
375 condition, representing nearly 50% of total As. From the end of the first incubation period,
376 dissolved As concentration remained very low but mainly in the form of AsV in the IN
377 microcosm. This result might be linked to the adsorption of AsIII followed by abiotic oxidation
378 at the surface of clay material (Lin and Puls, 2000).

379 **Table 1.** Total As, As speciation in the water phases of incubated slurries, and MPN of AsIII-
380 oxidising and AsV-reducing microbes.

Time	Condition	Total As (µg L^{-1})	AsIII (%)	AsV (%)	DMA^V (%)	Un. species 1* (%)	Un. species 2* (%)	Un. species 3* (%)	MPN AsIII-ox g^{-1} solids	MPN AsV-red g^{-1} solids
Beginning (T0m)	BIO A	17.0	40.0	60.0	ND	ND	ND	ND	< LQ	3.16×10^{3}
	BIO B	16.7	37.2	62.8	ND	ND	ND	ND	< LQ	3.76×10^{3}
	BIO C	15.3	36.9	63.1	ND	ND	ND	ND	8.00×10^{1}	9.20×10^{2}
	IN	14.3	95.5	4.5	ND	ND	ND	ND	< LQ	< LQ
End of first anaerobic period (T3m)	BIO A	155.0	4.8	0.8	ND	6.8	8.6	79.0	1.84×10^{3}	2.52×10^{3}
	BIO B	118.0	4.5	0.7	ND	9.8	7.9	77.0	9.60×10^{3}	5.20×10^{3}
	BIO C	141.0	6.7	1.3	ND	7.7	9.0	75.3	3.60×10^{3}	9.60×10^{4}
	IN	4.4	3.5	96.5	ND	ND	ND	ND	< LQ	< LQ
End of aerobic period (T6m)	BIO A	1.2	1.8	44.6	53.6	ND	ND	ND	5.20×10^{5}	9.60×10^{5}
	BIO B	1.4	1.5	46.2	52.3	ND	ND	ND	1.32×10^{5}	1.96×10^{5}
	BIO C	1.1	1.7	50	48.3	ND	ND	ND	1.32×10^{5}	5.20×10^{6}
	IN	0.5	4.0	95.0	1.0	ND	ND	ND	< LQ	< LQ
End of second anaerobic period (T9m)	BIO A	173.0	14.1	0.9	ND	10.3	5.9	68.8	1.96×10^{5}	3.68×10^{7}
	BIO B	278.0	88.7	2.3	ND	8.5	0.5	ND	9.60×10^{5}	6.80×10^{6}
	BIO C	193.0	25.7	1.6	ND	5.8	6.3	60.6	8.80×10^{5}	5.20×10^{6}
	IN	4.2	10.6	89.4	ND	ND	ND	ND	< LQ	< LQ

ND: not detected, (*) unidentified As-containing species, estimated indicative values calculated with AsV standard addition slope; LQ = 4.00×10^{1} g^{-1}.

Concentrations of Cl^{-}, Na^{+}, Ca^{2+} and Mg^{2+} remained stable and identical in BIO and IN conditions all along experiment (Supplementary Figure 6), whereas NO_3^{-} and SO_4^{2-} tended to be more impacted by redox conditions in BIO than in IN condition, particularly between T0m and T6m.

3.3.2. Microbial parameters

The quantification of As-transforming microbes by MPN showed the growth of active AsIII-oxidising and AsV-reducing bacteria throughout the incubation (Table 1), independently of aerobic or anaerobic periods, whereas in IN condition the quantity of As-transforming microbes remained lower than the quantification limit all along the experiment. AsV-reducing bacteria were always more abundant than AsIII-oxidising micro-organisms. At the end of the second anaerobic period, the order of magnitude of MPN in sediments from parallel microcosms A, B and C was 10^{6} g^{-1} for AsIII-oxidising bacteria and 10^{7} g^{-1} for AsV-reducing bacteria.

The PCA built with all physico-chemical and biological parameters measured during the incubation (Supplementary Figure 7) illustrates the contrast between the evolution of IN and BIO slurries. Arsenic concentration was correlated with Fe concentration, and negatively correlated with sulphate concentration. Moreover, this analysis suggests an early divergence, detectable at the end of the first incubation period, between the microcosm B and the two microcosms A and C.

The bacterial diversity in the slurries at the end of the second anaerobic period (supplementary Table 4) was higher than that of the groundwater bacterial communities, in spite of a lower richness. The corresponding 16S rRNA gene sequences (Fig. 5 E and F) showed close diversity

406 profiles in batches A and C, that differed from batch B that contained Euryarchaeota (Archaea
407 domain) in higher abundance, with a significant proportion of sequences affiliated to
408 methanogenic micro-organisms. All slurries contained, as major OTUs, sequences that were
409 only affiliated at the family level, first to Rhodocyclaceae, then to Geobacteraceae. Sum of
410 sulphate-reducers sequences (Supplementary Table 7) represented nearly 10% in A and C, but
411 only 0.3% in B. Conversely, sum of methanogens sequences represented 37% of the sequences
412 in B, but less than 0.2% in A and were not detected in C.

413

414 **4. Discussion**

415 *4.1. Geological context and origin of As in the confined aquifer*

416 Macroscopic and microscopic observations of the core material suggest that the sands and clays
417 covering the calcareous confined aquifer were deposited in a meandering river system
418 environment composed of channels, crevasse splay and floodplain facies. These last two facies
419 are enriched in As and other trace elements. The As enrichment in sedimentary facies linked
420 with high groundwater As concentrations was already reported (Chatterjee et al., 2003; Sahu
421 and Saha, 2015). In these formations, As-rich levels are generally described as containing
422 elevated organic matter concentrations. Here, the clayey levels presenting the highest As
423 contents displayed low organic carbon concentrations (0.01 to 0.02%). However, macroscopic
424 observation of plant debris in the core suggested that organic matter is present but distributed
425 in nuggets.

426

427 *4.2. As release mechanisms implying Fe and S cycles*

The geochemical composition of the confined groundwater, with absence of nitrate (< 0.5 mg L^{-1}) and presence of ammonium, dissolved Mn and Fe, suggests anaerobic conditions. The dissolved O_2 concentrations (0.9 to 2.3 mg L^{-1}) might be related to the diffusion of this gas into the well which creates local suboxic conditions. Low concentrations of SO_4^{2-} associated with high $\delta^{34}S$ of sulphate (mean of 16.3 ‰) would be consistent with in-situ sulphate reduction (Stueben et al., 2003; Wang et al., 2014). The evolution of the $\delta^{34}S_{SO4}$ of the water sampled in the drinking water well of Marcilly-en-Gault according to total sulphate concentration suggests variations of the in-situ activity of SRB, that might be influenced by evolution of redox conditions or organic matter supply. These $\delta^{34}S$ values are also associated to notable concentrations of As (mean 22.6 µg L^{-1}) as already described by various authors e. g., (Fig. 1C; Pi et al., 2018, Stueben et al., 2003, Wang et al., 2014). In a complementary way, the development of active As-transforming microbes during batch incubations confirmed the presence of living micro-organisms in the confined aquifer. These results support the hypothesis of active biogeochemical reactions influencing the release and speciation of As in groundwater.

A link between biogeochemical processes and As mobilisation from sediments to groundwater, implying diverse mechanisms and especially iron and sulphur cycles, was evidenced in several other sites. The mechanism most often at the origin of As release is the biological reduction of Fe oxides (Stuben et al., 2003; Zheng et al., 2004; Nath et al., 2009; Erickson et al., 2016; Ziegler et al., 2017; Johannesson et al., 2019). The confined groundwater of Marcilly-en-Gault contains dissolved Fe, the analysis of core materials indicated the presence of FeIII in the As-rich levels, and our slurry incubation experiment showed As and Fe release during anaerobic periods (Figure 5), and correlation between these two parameters (Supplementary Figure 7). These results support the hypothesis that Fe oxides reduction plays a major role in the release of As. Sulphate reduction was also invoked in previous studies as possibly contributing to As release through (1) indirect chemical reduction of Fe oxides by H_2S, and (2) the formation of

453 soluble thio-arsenate complexes (Wang et al., 2014; Gao et al., 2021). These processes might
454 have modestly contributed to As mobility in our microcosms. Pi et al. (2018) observed profiles
455 of biogeochemical Fe reduction and sulphate reduction controlling both As speciation and
456 concentration in groundwater of Datong basin, China. They hypothesised that vertical
457 variations of As concentrations and forms were associated with availability of organic matter,
458 providing energy to microbial reactions. Our incubations of core materials showed that bacterial
459 activities influenced As speciation, producing As species different from AsIII and AsV. In
460 anaerobic conditions, non-identified species might correspond to thio-arsenate complexes that
461 were already associated with bacterial sulphate reduction in core sediments microcosms (Gao
462 et al., 2021). In aerobic conditions, up to 50% of total As was present as DMA^V, a biologically
463 produced methylated species (Dombrowski et al., 2005). Yet, these species exclusively
464 produced when bacterial communities are active could be less efficiently adsorbed on Fe oxides
465 surfaces than AsV or AsIII (Lafferty and Loeppert, 2005; Couture et al., 2013). Thus, in
466 addition to the reduction of iron oxides, bio-reduction of sulphate and direct As transformation
467 by microbes could contribute to the mobility of this toxic element.

468

469 *4.3. Microbial assemblages*

470 *4.3.1. Groundwater*

471 The main major OTU found in Marcilly-en-Gault groundwater was affiliated to
472 Hydrogenophilaceae family, currently composed of 5 genera, *Thiobacillus*, *Hydrogenophilus*,
473 *Sulfuricella*, *Petrobacter*, and *Tepidiphilus* (Garrity et al., 2005; Orlygsson and Kristjansson,
474 2014). This family includes chemolithotrophic or mixotrophic bacteria able to oxidise inorganic
475 substrates, such as sulphur compounds or hydrogen, possibly using nitrate as electron acceptor
476 (*Sulfuricella*, Kojima and Fukui, 2010). The second main metabolic group found in

groundwater is composed of OTUs affiliated to Galliollenaceae, gathering autotrophic microorganisms oxidising FeII in micro-aerophilic environments. Their abundance in the sampled groundwater is consistent with the presence of dissolved Fe, and it might be assumed that they could form biofilms onto surfaces of the drinking water well (Stuetz and McLaughlan, 2004). They may also grow in areas of the aquifer where small quantities of oxygen could diffuse or be transported. Glodowska et al. (2021) already quantified non negligible proportions of Galliollenaceae and other putative FeII-oxidisers in As-bearing groundwater where they are assumed to favour As immobilisation with FeIII oxides formation in environments of low-oxygen availability. Bacteria that could contribute directly or indirectly to iron oxides reduction, such a sulphate reducers (Desulfurivibrionaceae) and FeIII reducers (*Georgfuchsia*) were always detected in groundwater samples, but in relatively low abundance. Interestingly, *Georgfuchsia* was described as able to degrade aromatic compounds (Weelink et al., 2009), that could be an asset to use organic molecules derived from buried plant debris. *Sphingopyxis*, another heterotroph found in the groundwater, is also known for its ability to degrade complex molecules (Sharma et al., 2021).

4.3.2. Batch experiments

The microbial communities retrieved at the end of the incubation experiment clearly differed from those observed in groundwater samples. This difference can be explained by the strong reducing conditions and hydrogen supply during the last incubation period, while in the drinking well, diffusion of oxygen could create microaerophilic conditions, specific to the local environment of this water source. Moreover, the sediment is a source of nutrients and carries some bacteria. Indeed, bacterial communities present in the water phase of aquifers may differ from those attached to solid phases (Smith et al., 2018). In these incubated slurries, the two most abundant OTUs were affiliated, at the family level, with Rhodocyclaceae and Geobacteraceae. Rhodocyclaceae family includes many genera presenting diverse

metabolisms; thus it is hardly possible to infer a role of members of this OTU. However, a recent report of microcosm experiment performed with groundwater and sediments supplied with hydrogen also led to enrichment of Rhodocyclaceae that could be related to the genus *Dechloromonas*, a hydrogenotrophic denitrifier (Duffner et al., 2021). This OTU was clearly enriched during incubation, but was also present in all groundwater samples, in small abundance. Geobacteraceae members share the ability to use FeIII as terminal electron acceptor and can use either small organic compounds or hydrogen as electron source (Röling, 2014). Their presence as a major OTU in our system can be related with the Fe oxides dissolution process which could mobilise As. This OTU was very rare in the groundwater samples, only sparsely detected in September 2016 and May 2018. Incubation also led to enrichment of Comamonadaceae, a very metabolically diverse family. The next groups of less abundant but major OTUs marked differences between microcosms: they included either SRB in A and C, or methanogens in B. This strong contrast between B compared with A/C microbial communities might be considered in the light of the difference in final geochemical profiles of the slurries: B presented much more dissolved Fe and As than A and C. In terms of sulphate concentrations, the three microcosms behaved similarly. The divergence of results in B might be linked to the initial heterogeneity of the solid phase inherent in the nature of the actual material that induced heterogeneity in initial microbial communities. Such phenomenon was previously reported in parallel slurries of underground sediment mixed with ferrihydrite (Kwon et al., 2016) which evolved differently in terms of geochemistry and microbial communities, this result being related with subtle differences in the initial composition of the microbial communities. High As concentrations in zones of active methanogenic activities have already been reported (Wang et al., 2015; Glodowska et al., 2021) whereas the biogeochemical link between methanogenesis and As release is not clearly elucidated. According to Glodowska et al. (2021), organic carbon input due to hydrogeological conditions fuels fermentation producing

hydrogen, thus, indirectly, methanogenic metabolisms and efficient reduction of As-bearing Fe minerals. Methane oxidation might also be coupled to FeIII reduction. In our systems, hydrogen was provided, thus could be consumed for both FeIII reduction and methanogenesis. One important question would be the possible availability of hydrogen or other electron donors in the confined aquifer. Previous studies showed that intrinsic organic matter of aquifer sediments could fuel anaerobic respiration processes (Duan et al., 2019; Gao et al., 2021). However, organic carbon concentration was very low in M8 sample, (0.02%) compared with that reported in previous studies (0.16 to 0.70% in Duan et al., 2019; 0.22% in Gao et al., 2021). The classical hypothesis of hydrogen production through fermentation of organic matter could hardly be considered in our system except if nuggets of organic matter, such as the plant debris macroscopically observed in the sedimentary profile, could be used as organic substrates. As a fact, the microbial community of incubated slurries contained the fermentative genus *Propionivibrio*, in low abundance (0.1 to 0.6%) but in all microcosms. Species of this genus, belonging to Rhodocyclaceae, are aerotolerant anaerobes performing fermentation of aromatic compounds (Brune et al., 2002); their emergence in the incubated slurries might indicate the intrinsic organic matter could be metabolised.

4.3.3. Linking microbial assemblages with biogeochemical processes

SRB were always detected both in groundwater samples and microcosms. However, they were present in relatively low abundance in groundwater, and in B microcosm in which the highest release of As was observed. In-situ evolution of SO_4 and $\delta^{34}S$ and the development of SRB in A and C slurries support the hypothesis of active sulphate-reduction in the confined aquifer.

Both groundwater and microcosms hosted microbial assemblages containing OTUs whose known members are involved in iron and sulphur cycles, but only a few methanogens except in one of the microcosms, where this metabolic group was abundant. All these types of microbial metabolisms were already observed in other As-bearing groundwater systems (Table 2).

552 Globally, the major abundance of bacterial OTUs involved in Fe cycling, i.e. FeII oxidation in
553 groundwater samples, and FeIII-reduction in all incubated slurries, strongly suggests a major
554 role of Fe biogeocyle in the confined aquifer. The Geobacteraceae-affiliated OTU massively
555 present at the end of slurry incubations, and putatively involved in Fe oxide reduction, was only
556 sparsely detected in groundwater samples, possibly because they were not mobile but attached
557 to solid phases, or because the local suboxic condition of the well was not suitable for their
558 growth. However another OTU, affiliated to *Georgfuchsia*, a known FeIII reducer (Weelink et
559 al., 2009), was present in low abundance but regularly along all seasons in groundwater.

560

561 **Table 2.** Main characters of microbial communities in arsenic-rich groundwater,
562 groundwater-related sediments, and related laboratory experiments

Environments	Main OTUs (16S genus level)	Main detected functions	References
Groundwater, Inner Mongolia	*Pseudomonas, Acinetobacter, Brevundimonas, Aquabacterium, Psychrobacter, **Geobacter**, Arthrobacter, Massilia, Dietzia, Sphingomonas, Planococcus, Methanosaeta, Nitrosophaera, Thermoprotei*	Not mentioned	Li et al., 2013
Holocene and Pleistocene sediments, Cambodia	***Geobacter**, Propionivibrio, Aeromonas, Acidobacteria, Pelagibius, Enterobacter, Pseudomonas, Sphingomonas, Pseudolabrys, Methylobacterium, Microvirga, Delftia, Tumebacillus, Euzebya, Dietzia*	Not mentioned	Hery et al., 2015

Groundwater, West Bengal, India	*Pseudomonas, Rhizobium, Brevundimonas, Rhodococcus, Rheinheimera, Phyllobacterium, Staphylococcus, Herbaspirillum, Acinetobacter, Arthrobacter, Bacillus, Stenotrophomonas, Hydrogenophaga*	As resistance, AsV respiration, AsIII oxidation, FeIII respiration, NO3 and SO4 respiration	Paul et al., 2015
Groundwater, Cremona, Italy	*Sphingopyxis, Sphingomonas, Thiobacillus, Methylophilus, Sulfuricurvum, Thiotrix, Pseudomonas, Azotobacter, Methylomonas Rhodobacter, Leptothrix,* ***Geobacter****, Geothrix, Ferribacterium*	AsIII oxidation, As resistance, AsV respiration (few), C fixation, FeIII-reduction	Cavalca et al., 2019
Groundwater, central Yangtze River Basin, China	*Sideroxydans, Gallionella,* ***Geobacter****, Methylotenera, Methylosinus, Methylomonas, Methylocaldum, Sulfurospirillum, Sulfuritaela, Methanospirillum, Methanosarcina, Methanosatea, Methanomassilicoccus, Methanobacterium, Desulfovibrio, Rhodoferax, Pseudomonas, Microbacterium, Flavobacterium, Aquabacterium, Acidovorax*	FeII oxidation, FeIII reduction	Zheng et al., 2019

Groundwater, Inner Mongolia		AsV respiration, As resistance	Wang et al., 2021
Groundwater, Central Yangtze River basin, China		SO_4 reduction (*dsr*B gene of *Desulfobulbus*, *Desulfocapsa*, *Desulfomonile*, *Desulfobacca*, *Desulfovibrio*, *Desulfurispora*, *Desulfatiglans*	Zheng et al., 2020
Groundwater, Sologne, France	***Gallionella,*** *Brevundimonas, Nitrospira,* ***Georgfuchsia****, Sphingopyxis, Perlucidibaca, Desulfurivibrio, Delftia, Sphingobium, Sediminibacterium, Magnetovibrio,* ***Ferriphaselus***	AsIII-oxidation, AsV-reduction	Present study
Incubations with lactate + acetate, Holocene and Pleistocene sediments, Cambodia	***Geobacter****, Sulfurospirillum, Desulfovibrio Pelosinus, Hydrogenophaga, Dechloromonas, Desulfobulbaceae*	AsV respiration	Hery et al., 2015
Microcosms, Jianghan Plain, China	*Pseudomonas, Pedobacter, Paenibacillus, Cellulomonas, Clostridium, Thiobacillus,* ***Geobacter****, Dechloromonas, Desulfosporosinus, Clostridium*	Sulphate reduction, FeIII-reduction, As resistance	Deng et al., 2018

Microcosms	*Desulfovibrio, Desulfomicrobium,* ***Geobacter****, Methanosarcina, Methanobacterium*	Sulphate-reduction, AsV respiration	Gao et al., 2021
Microcosms, Sologne, France	*Methanobacterium, Desulfovibrio, Sediminibacterium, Thermincola, Sulfuritalea, Lacibacter, Propionivibrio, Haliangium, Methyloversatilis, Sandaracinus*	AsIII-oxidation, AsV-reduction	Present study

5. Conclusion

The occurrence of As in the confined aquifer of Sologne appears to find its origins in anoxic bioprocesses, as already described in other sedimentary paleo-environments. In particular, the Fe oxides detected in As-rich floodplain and crevasse splay clays (fluvial environment) covering the calcareous aquifer (lake environment) could be biologically reduced. The major role of FeIII reduction in As release was supported by high Fe concentrations in water and solid phases, and proportions of microbial groups involved in Fe bio-geocycle, both in groundwater samples and microcosms. Other microbial reactions could play non negligible roles in As mobilisation, namely sulphate reduction, AsV reduction, AsIII oxidation and As methylation. Corresponding bacterial activities drive the production of diverse As species whose proportions may fluctuate and influence the distribution of As between solids and water. Even if phenomena globally followed the same patterns in all microcosms, our results underline the possibility of strong variations in the amplitude of the bio-reactions driving As release from solids to water, linked to subtle heterogeneities that induced important divergence of microbial communities compositions. This phenomenon, generally ignored or underestimated, deserves to be explored further to improve the accuracy of predictive models taking into account biogeochemical

reactions. In the context of global change and increasing anthropic pressure on water resources, managers will need reliable tools to anticipate the evolution of groundwater quality. At larger scale, important spatial heterogeneities of organic matter distribution and As concentrations, linked to geological context, i.e. sedimentary deposition in the meandering river system (channels, crevasse splay and floodplain), may occur and induce local variations of the intensity of biogeochemical processes. The mechanisms of As release in the sub-surface and their potential evolution with groundwater table level would need to be better understood through long-term monitoring of dissolved As species, and development of experimental systems and models taking into account heterogeneities at different scales.

Acknowledgements

This research was supported by the Water Agency Loire-Bretagne (decision n°2015C009), and by BRGM funding PEX BIODIV. We thank Luigi Ardito for performing core sampling operation, and the municipal authority of Marcilly-en-Gault for allowing our sampling campaigns.

References

Bassil, J., Naveau, A., Bueno, M. Di Tullo, P., Grasset, L., Kazpard, V., Razack, M., 2016. Determination of the distribution and speciation of selenium in argillaceous sample using chemical extractions and post-extractions analyses: application to the hydrogeological experimental site of Poitiers. Environ. Sci. Pollut. Res. 23, 9598-9613. https://doi.org/10.1007/s11356-016-6113-7

Borcard, D., Gillet, F., Legendre, P., 2011. Numerical ecology with R. Vol. 2. p. 688. Springer, New York.

603 Brune, A., Ludwig, W., Schink, B., 2002. *Propionivibrio limicola* sp. nov., a fermentative bacterium
604 specialized in the degradation of hydroaromatic compounds, reclassification of *Propionibacter*
605 *pelophilus* as *Propionivibrio pelophilus* comb. nov. and amended description of the genus
606 *Propionivibrio*. Int. J. Syst. Evol. Microbiol. 52 (2), 441–444. https://doi.org/10.1099/00207713-52-2-
607 441

608 Cary, L., Klinka, T., Battaglia-Brunet, F., 2018. Contexte, origines et biogéochimie de l'arsenic et du
609 sélénium dans la nappe des calcaires de Beauce - Base de données des informations régionales
610 disponibles et SIG. Rapport intermédiaire. BRGM/RP-67429-FR, http://infoterre.brgm.fr

611 Cavalca, L., Zecchin, S., Zaccheo, P., Abbas, B., Rotiroti, M., Bonomi, T., Muyzer, G., 2019. Exploring
612 Biodiversity and Arsenic Metabolism of Microbiota Inhabiting Arsenic-Rich Groundwaters in Northern
613 Italy. Front. Microbiol. 10, 1480. https://doi.org/10.3389/fmicb.2019.01480

614 Chakraborti, D., Rahman, M.M., Ahamed, S., Dutta, R.N., Pati, S., Mukherjee, S.C., 2016. Arsenic
615 groundwater contamination and its health effects in Patna district (capital of Bihar) in the middle Ganga
616 plain, India. Chemosphere 152, 520-529. https://doi.org/10.1016/j.chemosphere.2016.02.119

617 Chatterjee, D., Chakraborty, S., Nath, B., Jana, J., Bhattacharyya, R., Mallik, S.B., Charlet, L., 2003.
618 Mobilization of arsenic in sedimentary aquifer vis-à-vis subsurface iron reduction processes. J. Phys. IV
619 France 107 (2003) 293. https://doi.org/10.1051/jp4:20030299

620 Chung, F.H., 1974. Quantitative interpretation of X-ray diffraction patterns of mixtures. I. matrix-
621 flushing method for quantitative multicomponent analysis. J. Appl. Cryst. 7, 519-52.
622 https://doi.org/10.1107/S0021889874010375

623 Couture, R.M., Rose, J., Kumar, N., Mitchell, K., Wallschläger, D., Van Cappellen, P., 2013. Sorption
624 of Arsenite, Arsenate, and Thioarsenates to Iron Oxides and Iron Sulfides: A Kinetic and Spectroscopic
625 Investigation. Environ. Sci. Technol. 47 (11), 5652−5659. https://doi.org/10.1021/es3049724

626 Deng, Y., Zheng, T., Wang, Y., Liu, L., Jiang, H., Ma, T., 2018. Effect of microbially mediated iron
627 mineral transformation on temporal variation of arsenic in the Pleistocene aquifers of the central Yangtze
628 River basin. Sci. Total Environ. 619–620,1247-1258. https://doi.org/10.1016/j.scitotenv.2017.11.166

629 Desprez, N., Martin, C., 1970. Hydrogéologie du calcaire de Beauce sous la Sologne (Loiret Loir-et-
630 Cher). BRGM/70-SGN-023-BDP. http://pmb.brgm.fr/brgm/brgm_broogle_notice.php?id=30075

631 Dombrowski, P.M., Long, W., Farley, K.J., Mahony, J.D., Capitani, J.F., Di Toro, D.M., 2005.
632 Thermodynamic Analysis of Arsenic Methylation. Environ. Sci. Technol. 39 (7), 2169–76.
633 https://doi.org/10.1021/es0489691

634 Duan, Y., Schaefer, M.V., Wanga, Y., Gan, Y., Yua, K., Deng, Y., Fendorf, S., 2019. Experimental
635 constraints on redox-induced arsenic release and retention from aquifer sediments in the central Yangtze
636 River Basin. Sci. Total Environ. 649, 629-639. https://doi.org/10.1016/j.scitotenv.2018.08.205

637 Duffner, C., Holzapfel, S., Wunderlich, A., Einsiedl, F., Schloter, M., Schulz, S., 2021. *Dechloromonas*
638 and close relatives prevail during hydrogenotrophic denitrification in stimulated microcosms with oxic
639 aquifer material, FEMS Microbiol. Ecol. 97 (3), fiab004, https://doi.org/10.1093/femsec/fiab004

640 Erickson, M.L., Yager, R.M., Kauffman, L.J., Wilson, J.T., 2019. Drinking water quality in the glacial
641 aquifer system, northern USA. Sci. Tot. Environ., 694, 133735.
642 https://doi.org/10.1016/j.scitotenv.2019.133735

643 Erickson, M.L., Ziegler, B.A., 2016. Arsenic Cycling in Hydrocarbon Plumes: Secondary Effects of
644 Natural Attenuation. Groundwater, 54, 35-45. https://doi.org/10.1111/gwat.1231

645 Escudié, F., Auer, L., Bernard, M., Mariadassou, M., Cauquil, L., Vidal, K., Maman, S., Hernandez-
646 Raquet, G., Combes, S., Pascal, G., 2018. FROGS: Find, Rapidly, OTUs with Galaxy Solution.
647 Bioinformatics 34, 1287–1294. https://doi.org/10.1093/bioinformatics/btx791

648 EU Council Directive 98/83/EC of 3 November 1998 on the quality of water intended for human
649 consumption.

650 Fernandez-Rojo, L., Héry, M., Le Pape, P., Braungardt, C., Desoeuvre, A., Torres, E., Tardy, V.,
651 Resongles, E., Laroche, E., Delpoux, S., Joulian, C., Battaglia-Brunet, F., Boisson, J., Grapin, G., Morin,
652 G., Casiot, C., 2017. Biological attenuation of arsenic and iron in a continuous flow bioreactor treating
653 acid mine drainage (AMD). Wat. Res. 123, 594-606. https://doi.org//10.1016/j.watres.2017.06.059

654 Gao, J., Zheng, T., Deng, Y., Jiang, H., 2021. Microbially mediated mobilization of arsenic from aquifer
655 sediments under bacterial sulfate reduction. Sci. Total Environ. 768, 144709.
656 https://doi.org/10.1016/j.scitotenv.2020.144709

657 Garrity, G.M., Bell, J.A., Lilburn, T., 2005. Order II. *Hydrogenophilales* ord. nov., in: Brenner, D.J.,
658 Krieg, N.R., Staley, J.T., Garrity, G.M. (Eds.), Bergey's Manual of Systematic Bacteriology, vol. 2: The
659 Proteobacteria, part C (The Alpha-, Beta-, Delta-, and Epsilonproteobacteria), New York, Springer,
660 2005, 2e éd., 763 p.

661 Gillispie, E.C., Andujar, E., Polizzotto, M.L., 2016. Chemical controls on abiotic and biotic release of
662 geogenic arsenic from Pleistocene aquifer sediments to groundwater. Environ. Sci.: Processes
663 Impacts, 18, 1090. https://doi.org/10.1039/c6em00359arsc.li/process-impacts

664 Glodowska, M., Stopelli, E., Straub, D., Thi, D.V., Trang, P.T.K., Viet, P.H., Berg, M., Kappler, A.,
665 Kleindienst, S., 2021. Arsenic behavior in groundwater in Hanoi (Vietnam) influenced by a complex
666 biogeochemical network of iron, methane, and sulfur cycling. J. Haz. Mat. 407, 124398.
667 https://doi.org/10.1016/j.jhazmat.2020.124398

668 Hallbeck, L., Pedersen, K., 2014. The Family *Gallionellaceae*, in: Rosenberg, E., DeLong, E.F.,
669 Lory, S., Stackebrandt, E., Thompson, F. (Eds), The Prokaryotes. Springer, Berlin, Heidelberg.
670 https://doi.org/10.1007/978-3-642-30197-1_398

671 Héry, M., Rizoulis, A., Sanguin, H., Cooke, D.A., Pancost, R.D., Polya, D.A., Lloyd, J.R., 2015. As
672 mobilization in contrasting Cambodian sediments. Environ. Microbiol. 17 (6), 1857-1869.
673 https://doi.org/10.1111/1462-2920.12412

Johannesson, K.H., Yang, N., Trahan, A.S., Telfeyan, K.T., Mohajerin, J., Adebayo, S.B., Akintomide, O.A., Chevis, D.A., Datta, S., White, C.D., 2019. Biogeochemical and reactive transport modeling of arsenic in groundwaters from the Mississippi River delta plain: An analog for the As-affected aquifers of South and Southeast Asia. Geochim. Cosmochim. Act. 264, 245-272. https://doi.org/10.1016/j.gca.2019.07.032

Kim, M.J., 2001. Separation of inorganic arsenic species in groundwater using ion exchange method. Bull. Environ. Contam. Toxicol. 67, 46-51. https://doi.org/10.1007/s001280089

Kloppmann, W., Negev, I., Guttman, J., Goren, O., Gavrieli, I., Guerrot, C., Flehoc, C., Pettenati, M., Burg, A., 2018. Massive arrival of desalinated seawater in a regional urban water cycle: A multi-isotope study (B, S, O, H). Sci. Total Environ. 619–620, 272-280. https://doi.org/10.1016/j.scitotenv.2017.10.181

Kojima, H., Fukui, M., 2010. *Sulfuricella denitrificans* gen. nov., sp. nov., a sulfur-oxidizing autotroph isolated from a freshwater lake. Int. J. Syst. Evol. Microbiol. 60 (12), 2862-2866. https://doi.org/10.1099/ijs.0.016980-0

Kwon, M.J., O'Loughlin, E.J., Boyanov, M.I., Brulc, J.M., Johnston, E.R., Kemner, K.M., Antonopoulos D.A., 2016. Impact of Organic Carbon Electron Donors on Microbial Community Development under Iron- and Sulfate-Reducing Conditions. PLOS ONE. https://doi.org/10.1371/journal.pone.0146689

Lafferty, B.J., Loeppert, R.H., 2005. Methyl Arsenic Adsorption and Desorption Behavior on Iron Oxides. Environ. Sci. Technol. 39 (7), 2120-2127. https://doi.org/10.1021/es048701

Li, P., Wang, Y., Jiang, Z., Jiang, H., Li, B., Dong, H., Wang, Y., 2013. Microbial Diversity in High Arsenic Groundwater in Hetao Basin of Inner Mongolia, China. Geomicrobiol. J. 30 (10), 897-909. https://doi.org/10.1080/01490451.2013.791354

Michel, C., Baran, N., André, L., Charron, M., Joulian, C., 2021. Side effects of pesticides and metabolites in groundwater: Impact on denitrification. Front. Microbiol. 12, 662727. https://doi.org/10.3389/fmicb.2021.662727

Nath, B., Chakraborty, S., Burnol, A., Stüben, D., Chatterjee, D., Charlet, L., 2009. Mobility of arsenic in the sub-surface environment: An integrated hydrogeochemical study and sorption model of the sandy aquifer materials, J. Hydrol. 364 (3-4), 236-248. https://doi.org/10.1016/j.jhydrol.2008.10.025

Orlygsson, J., Kristjansson, J.K., 2014. The Family *Hydrogenophilaceae*, in: Rosenberg, E., DeLong, E.F., Lory, S., Stackebrandt, E., Thompson, F. (Eds), The Prokaryotes. Springer, Berlin, Heidelberg. https://doi.org/10.1007/978-3-642-30197-1_244Paul, D., Kazy, S.K., Banerjee, T.D., Gupta, A.K., Pal, T., Sar, P., 2015. Arsenic biotransformation and release by bacteria indigenous to arsenic contaminated groundwater. Biores. Technol. 188, 14-23. https://doi.org/10.1016/j.biortech.2015.02.039

Pi, K., Wang, Y., Postma, D., Ma, T., Su, C., Xie, X., 2018. Vertical variability of arsenic concentrations under the control of iron-sulfur-arsenic interactions in reducing aquifer systems. J. Hydrol. 561, 200-210. https://doi.org/10.1016/j.jhydrol.2018.03.049

Podgorski, J., Berg, M., 2020. Global threat of arsenic in groundwater. Science, 368 (6493), 845-850. https://doi.org/10.1126/science.aba1510Poirel, J., Joulian, C., Leyval, C., Billard, P., 2013. Arsenite-induced changes in abundance and expression of arsenite transporter and arsenite oxidase genes of a soil microbial community. Res. Microbiol. 164 (5), 457-65. https://doi.org/10.1016/j.resmic.2013.01.012

Radloff, K.A., Cheng, Z., Rahman, M.W., Ahmed, K.M., Mailloux, B.J., Juhl, A.R., Schlosser, P., van Geen, A., 2007. Mobilization of Arsenic During One-Year Incubations of Grey Aquifer Sands from Araihazar, Bangladesh. Environ. Sci. Technol. 41 (10), 3639–3645. https://doi.org/10.1021/es062903j

Ravenscroft, P., Brammer, H., Richards, K., 2009. Arsenic Pollution: A Global Synthesis, RGS-IBG Book Series, A John Wiley and Sons Ltd. Publication, London.

Röling, W.F.M., 2014. The Family *Geobacteraceae*, in: Rosenberg, E., DeLong, E.F., Lory, S., Stackebrandt, E., Thompson, F. (Eds.), The Prokaryotes. Springer, Berlin, Heidelberg. https://doi.org/10.1007/978-3-642-39044-9_381

Roy, J.S., Chatterjee, D., Das, N. et al., 2018. Substantial Evidences Indicate That Inorganic Arsenic Is a Genotoxic Carcinogen: a Review. Toxicol. Res. 34, 311–324. https://doi.org/10.5487/TR.2018.34.4.311

Sahu, S., Saha, D., 2015. Role of shallow alluvial stratigraphy and Holocene geomorphology on groundwater arsenic contamination in the Middle Ganga Plain, India. Environ. Earth. Sci. 73, 3523–3536. https://doi.org/10.1007/s12665-014-3637-3

Schaefer, M.V., Ying, S.C., Benner, S.G., Duan, Y., Wang, Y., Fendorf, S., 2016. Aquifer Arsenic Cycling Induced by Seasonal Hydrologic Changes within the Yangtze River Basin. Env. Sci. Technol. 50 (7), 3521−3529. https://doi.org/10.1021/acs.est.5b04986

Schmidt, C.W., 2014. Low-dose arsenic: in search of a risk threshold. Env. Health Perspect. 122 (5), A131–4. https://doi.org/10.1289/ehp.122-A130

Schuhmacher-Wolz, U., Dieter, H.H., Klein, D., Schneider, K., 2009. Oral exposure to inorganic arsenic: evalution of its carcinogenic and non-carcinogenic effects. Crit. Rev. Toxicol. 39 (4), 271-298. https://doi.org/10.1080/10408440802291505

Stuben, D., Berner, Z., Chandrasekharam, D., Karmakar, J., 2003. Arsenic enrichment in groundwater of West Bengal, India: geochemical evidence for mobilization of As under reducing conditions. Appl. Geochem. 18 (9), 1417–1434. https://doi.org/10.1016/S0883-2927(03)00060-X

Sharma, M., Khurana, H., Narain, S.D., Negi, R.K., 2021. The genus *Sphingopyxis*: Systematics, ecology, and bioremediation potential - A review, J. Environ. Manage., 280, 111744. https://doi.org/10.1016/j.jenvman.2020.111744

Smith, H.J., Zelaya, A.J., De Le´on, K.B., Chakraborty, R., Elias, D.A., Hazen, T.C., Arkin, A.P., Cunningham, A.B., Fields, M.W., 2018. Impact of hydrologic boundaries on microbial planktonic and

biofilm communities in shallow terrestrial subsurface environments. FEMS Microbiol. Ecol. 94, fiy191. https://doi.org/10.1093/femsec/fiy191

Stuetz, R.M., McLaughlan, R.G., 2004. Impact of localised dissolved iron concentrations on the biofouling of environmental wells. Wat. Sci. Technol. 49 (2), 107–113. https://doi.org/10.2166/wst.2004.0100

Thouin, H., Le Forestier, L., Gautret, P., Hube, D., Laperche, V., Dupraz, S., Battaglia-Brunet, F., 2016. Characterization and mobility of arsenic and heavy metals in soils polluted by the destruction of arsenic-containing shells from the Great War. Sci. Total Environ. 550, 658–669. https://doi.org/10.1016/j.scitotenv.2016.01.111

Thouin, H., Battaglia-Brunet, F., Norini, M.P., Le Forestier, L., Charron, M., Dupraz, S., Gautret, P., 2018. Influence of environmental changes on the biogeochemistry of arsenic in a soil polluted by the destruction of chemical weapons: a mesocosm study. Sci. Total Environ. 627, 216-226. https://doi.org/10.1016/j.scitotenv.2018.01.158

Tsuji, J.S., Chang, E.T., Gentry, P.R., Clewell, H.J., Boffetta, P., Cohen, S.M., 2019. Dose-response for assessing the cancer risk of inorganic arsenic in drinking water: the scientific basis for use of a threshold approach, Crit. Rev. Toxicol. 49 (1,) 36-84, https://doi.org/10.1080/10408444.2019.1573804

Wang, Y., Morimoto, S., Ogawa, N., Oomori, T., Fujii, T., 2009. An improved method to extract RNA from soil with efficient removal of humic acids. J. Appl. Microbiol. 107, 1168–1177. https://doi.org/10.1111/j.1365-2672.2009.04298.xWang, Y., Xie, X., Johnson, T.M., Lundstrom, C.C., Ellis, A., Wang, X., Duan, M., Li, J., 2014. Coupled iron, sulfur and carbon isotope evidences for arsenic enrichment in groundwater. J. Hydrol. 519 (A), 414-422. https://doi.org/10.1016/j.jhydrol.2014.07.028

Wang, Y.H., Li, P., Dai, X.Y., Zhang, R., Jiang, Z., Jiang, D.W., Wang, Y.X., 2015. Abundance and diversity of methanogens: Potential role in high arsenic groundwater in Hetao Plain of Inner Mongolia, China. Sci. Total Environ., 515–516: 153-161. https://doi.org/10.1016/j.scitotenv.2015.01.031

769 Wang, J., Zeng, X.C., Zhu, X., Chen, X., Zeng, X., Mu, Y., Yang, Y., Wang, Y., 2017. Sulfate enhances
770 the dissimilatory arsenate-respiring prokaryotes-mediated mobilization, reduction and release of
771 insoluble arsenic and iron from the arsenic-rich sediments into groundwater. J. Haz. Mat. 339 (5), 409-
772 417. https://doi.org/10.1016/j.jhazmat.2017.06.052

773 Wang, Y., Wei, D., Li, P., Jiang, Z., Liu, H., Qing, C., Wang, H., 2021. Diversity and arsenic-
774 metabolizing gene clusters of indigenous arsenate-reducing bacteria in high arsenic groundwater of the
775 Hetao Plain, Inner Mongolia. Ecotox. 30, 1680–1688. https://doi.org/10.1007/s10646-020-02305-
776 1Weelink, S.A., van Doesburg, W., Saia, F.T., Rijpstra, W.I., Röling, W.F., Smidt, H., Stams, A.J.,
777 2009. A strictly anaerobic betaproteobacterium *Georgfuchsia toluolica* gen. nov., sp. nov. degrades
778 aromatic compounds with Fe(III), Mn(IV) or nitrate as an electron acceptor. FEMS Microbiol. Ecol.
779 70(3), 575-85. https://doi.org/10.1111/j.1574-6941.2009.00778.x

780 Welch, A.H., Westjohn, D.B., Helsel, D.R., Wanty, R.B., 2000. Arsenic in ground water of the United
781 States: occurrence and geochemistry. USGS Publications Warehouse.
782 http://pubs.er.usgs.gov/publication/70022646

783 Ziegler, B.A., Schreiber, M.E., Cozzarelli, I.M., Crystal Ng, G.H., 2017. A mass balance approach to
784 investigate arsenic cycling in a petroleum plume. Env. Poll. 231, 1351-1361.
785 https://doi.org/10.1016/j.envpol.2017.08.110

786 Zheng, Y., Stute, M., van Geen, A., Gavrieli, I., Dhara, R., Simpson, H.J., Schlosser, P., Ahmed, K.M.,
787 2004. Redox control of arsenic mobilization in Bangladesh groundwater. Appl. Geochem. 19 (2), 201–
788 214. https://doi.org/10.1016/j.apgeochem.2003.09.007

789 Zheng, T., Deng, Y., Wang, Y., Jiang, H., O'Loughlin, E.J., Flynn, T.M., Gan, Y., Ma, T., 2019.
790 Seasonal microbial variation accounts for arsenic dynamics in shallow alluvial aquifer systems. J. Haz.
791 Mat. 367 (5), 109-119. https://doi.org/10.1016/j.jhazmat.2018.12.087

792 Zheng, T., Deng, Y., Wang, Y., Jiang, H., Xie, X., Gan, Y., 2020. Microbial sulfate reduction facilitates
793 seasonal variation of arsenic concentration in groundwater of Jianghan Plain, Central China. Sci. Total
794 Environ. 735, 139327. https://doi.org/10.1016/j.scitotenv.2020.139327

795 Zuzolo, D., Cicchella, D., Demetriades, A., Birke, M., Albanese, S., Dinelli, E., Lima, A., Valera, P.,
796 De Vivo, B., 2020. Arsenic: Geochemical distribution and age-related health risk in Italy. Env. Res. 182,
797 109076. https://doi.org/10.1016/j.envres.2019.109076

HIGHLIGHTS

- Arsenic of sedimentary origin influences quality of a French groundwater
- Temporal variations of As- and S- cycles bio-indicators are observed on site
- Incubations of core material show biologically related As solubilisation
- Incubated core slurries and groundwater present distinct bacterial communities
- As concentration and speciation is driven by bacterial activities

Declaration of competing interest

The authors declare that they have no known competing interest that could have influenced this research results and interpretation.